Application of STATCOM to improve the LVRT of DFIG during RSC Fire-through Fault

A. F. Abdou , *Student Member IEEE,* A. Abu-Siada, *Senior Member IEEE* and H. R. Pota, *Member IEEE*

***Abstract*—The use of doubly fed induction generators (DFIGs) in large wind energy conversion systems (WECS) has significantly increased during the last few years. The DFIG is interfaced to the AC network through a grid side voltage source converter (GSC) and a rotor side voltage source converter (RSC) to enable the variable speed operation of the wind turbine. Moreover, it provides reactive power support to the AC grid during disturbances. The sensitivity of DFIGs to external faults has motivated researchers to investigate the impact of various grid disturbances, such as voltage sag and short circuit faults, on the low voltage ride through (LVRT) capability of DFIGs. However, no attempts have been made to investigate the impact of converter internal faults on the LVRT of the DFIG-based WECS. In this paper, the impact of a fire-through fault when it occurs in the RSC on the DC-capacitor voltage, rotor current, and the LVRT capability of the DFIG is investigated. A STATCOM controller to mitigate the effects of this fault is proposed. The DFIG compliance with various recently released LVRT grid codes under the fire-through fault with and without the STATCOM is examined and compared. Simulation results indicate that fire-through fault has a severe impact on the DFIG voltage profile and the proposed controller is capable of bringing the voltage profile at the point of common coupling (PCC) to the nominal steady state level.**

***Index Terms*—DFIG, Fire-Through, STATCOM, LVRT, VSC, RSC, GSC, Grid codes.**

I. Introduction

THE use of wind energy is growing rapidly and it is expected to provide ten percent of the global electricity generation by the year 2020 [1]. Among variable speed constant-frequency wind turbines, the doubly fed induction generator (DFIG) has been a popular candidate in the wind energy conversion systems (WECS) due to its advantages [2-5]. When compared to fixed-speed induction generators, the DFIG has the advantages of maximum power capture, less mechanical stresses, and less acoustical noise [3]. Compared with the full-converter variable-speed generators, the DFIG is a preferable choice in terms of size, cost, reduced losses and weight associated with the small converter [6]. The voltage source converters (VSCs) that interface the DFIG and the AC grid are rated at 30% of the generator power capacity for a rotor speed range of ±30% [7]. As the rotor side converter (RSC) operates at a low slip frequency range of ±30% of the line frequency, it can cause a high temperature variation and the power cycling capability of the IGBT bond wire can be reduced dramatically [8], and the whole IGBT-based system may easily fail [9]. Any problems caused to the IGBT or the controller circuit may result in rotor over-current. The common solution to protect the converter switches from DFIG rotor over-current is by connecting a crowbar circuit across the rotor terminals to isolate the converter from the rotor when rotor current exceeds the maximum safety margin.

Statistical surveys indicate that about 38% of power converter failures are due to converter switches while 53% of their failures are attributed to faults within converter control circuits [10, 11]. A recent industry-based survey concludes that the gate control circuits are the most susceptible components in converter faults [12]. Voltage source converters are subject to common faults such as fire-through, and flashover [13-17]. These faults can be caused by various malfunctions in the control and firing equipment [14, 17]. Fire-through is the conduction of a switch before its programmed instant of conduction [14, 16]. Although most internal converter faults are self-healed when the cause of these faults is of a transient nature [16], they can still have a detrimental impact on the overall performance of the DFIG-based WECS. Researchers have given attention to the dynamic performance of the DFIG-based WECS during various grid disturbances such as load fluctuation, voltage sag and swell, and short circuit faults on the grid side [18-24]. There are some studies that have investigated the effect of internal converter faults on the performance of HVDC systems [25-27]. However, no attention has been given to investigating the impact of such fault on the performance of the DFIG-based WECS and its compliance to the recently developed grid codes.

Flexible AC transmission systems (FACTS) based power electronic converters such as static synchronous compensator (STATCOM) are currently being used extensively in power system applications because of their ability to provide flexible power flow control [28, 29]. A STATCOM has the ability to provide reactive power during voltage collapse with rapid response as it has no delay associated with the thyristor firing [30].

This paper investigates the impact of the fire-through fault on the DC-capacitor voltage, rotor current, and the LVRT capability of the DFIG when it takes place within the RSC. Compliance of the DFIG performance under fire-through fault with the LVRT codes of various recent grid codes is also investigated. A STATCOM controller is proposed to mitigate the impact of these faults and to maintain the PCC voltage

A. F. Abdou and H. R. Pota are with the School of SEIT, UNSW@ADFA, Canberra, Australia (e-mail: a.abdou@adfa.edu.au) and (e-mail: h.pota@adfa.edu.au).
A. Abu-Siada is with the Department of Electrical and Computer Engineering, Curtin University, Perth, WA 6845 Australia (e-mail: a.abusiada@curtin.edu.au).

constant through the fault duration and after the fault clearance.

II. System Under Study

The single machine infinite bus (SMIB) system, shown in Fig. 1, is simulated using the EMTDC/PSCAD software to perform the investigations proposed in this paper. The DFIG stator terminals are connected to the grid through a coupling transformer and a short transmission line. The rotor windings are fed through back-to-back IGBT-based voltage source converters with a common DC-link capacitor and chopper to limit the capacitor over voltage. The DFIG grid side converter (GSC) and rotor side converter (RSC) are controlled by a four quadrant vector control as detailed in [31, 32] and is briefly elaborated below.

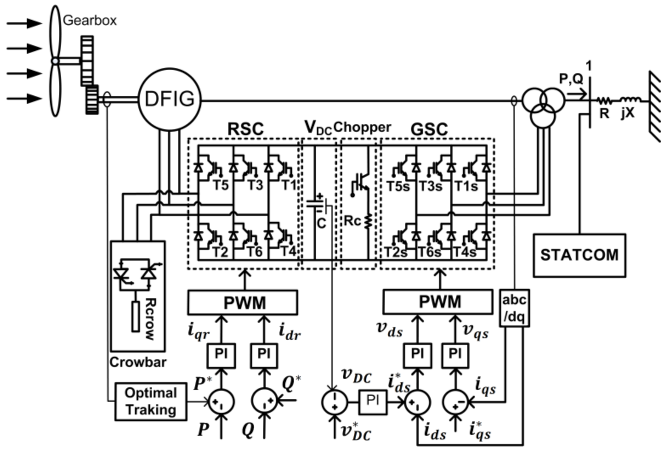

Fig. 1 Single line diagram of the system under study

A. GSC PWM Vector Control

The main task for GSC is to control the power exchange between AC grid and the dc-link to maintain the DC-voltage across the capacitor within permissible levels. In this context, a proper reference level for the d-axis stator current i^*_{ds} is created using the voltage error signal across the DC-link capacitor as an input to a proportional-integral (PI) controller while the q-axis reference current i^*_{qs} is assumed to be zero. Clarke-Park transformation [3] is used to convert the stator terminal currents from the a-b-c reference frame to the d-q reference frame (i_{ds} and i_{qs}) as shown in Fig. 1. The error signals of the stator d- and q- axes currents are used along with PI controllers to create appropriate d-q reference signals for stator voltages (v_{ds} and v_{qs}) that are used as inputs to the GSC pulse width modulation (PWM) circuit to create appropriate firing pulses to the GSC switches.

B. RSC PWM Vector Control

The RSC controls the generated active power according to the wind speed and the wind turbine characteristics while the reactive power command is set according to the utility requirements. A reference power P^* is selected based on the wind turbine characteristics to track the maximum power, and it is compared with the measured output power to create an error signal that is fed to a PI controller to generate the q-axis rotor current i_{qr}. To achieve unity power factor operation, the reactive power reference is set to zero and is compared with the measured value to create an error signal that is fed to another PI controller to generate the rotor d-axis current i_{dr}. Currents i_{qr} and i_{dr} are used as inputs to the RSC PWM circuit to create appropriate firing pulses to the RSC switches.

III. STATCOM Modeling

STATCOM is a shunt-connected reactive power compensation device that is capable of generating or absorbing reactive power. The STATCOM has three main components: voltage source converter (VSC), coupling transformer and the control circuit. The VSC is modeled as a six-pulse PWM GTO converter with a DC-link capacitor. The interaction between the AC system voltage and the voltage at the STATCOM terminals controls the reactive power flow. If the system voltage is less than the voltage at the STATCOM terminals, the STATCOM acts as a capacitor and reactive power is injected from the STATCOM to the system. On the other hand, if the system voltage is higher than the voltage at the STATCOM terminal, the STATCOM behaves as an inductor and the reactive power transfers from the system to the STATCOM. Under normal operating conditions, both voltages are equal and there is no power exchange between the STATCOM and the AC system.

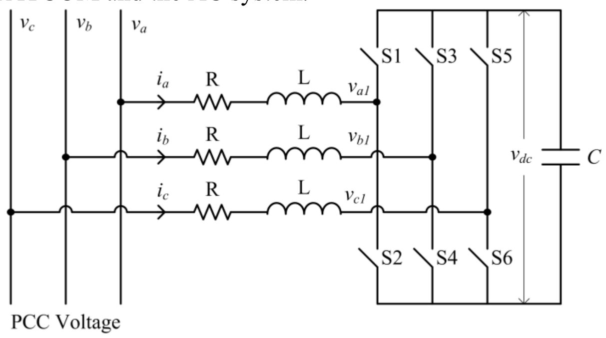

Fig. 2 The equivalent circuit of the STATCOM

The active and the reactive power exchange between the STATCOM and the AC system is controlled via the VSC firing angle α and the modulation index m to maintain the voltage at the point of connection and the DC-voltage within permissible limits.

A PI controller with the non-linear model of The STATCOM is used as detailed below:

Fig. 2 shows the STATCOM connected to the PCC in three-phase form, the differential equations for Fig. 2 in three-phase form can be written as

$$L\frac{di_a}{dt} = -Ri_a + (v_a - v_{a1})$$
$$L\frac{di_b}{dt} = -Ri_b + (v_b - v_{b1}) \quad (1)$$
$$L\frac{di_c}{dt} = -Ri_c + (v_c - v_{c1})$$

where i_a, i_b, and i_c are the AC line currents of the STATCOM; v_a, v_b, and v_c are the PCC voltages; v_{a1}, v_{b1}, and v_{c1} are the inverter terminal voltages; R and L represent the equivalent conduction losses and the inductance for the transformer and the filter.

By considering the system parameters and the system voltages as a three-phase balanced system, the three-phase voltages and currents can be converted into a synchronously rotating d-q frame. Equation (3) can be represented in the d-q frame as following:

$$L\frac{di_d}{dt} = -Ri_d + \omega L i_q + (v_d - v_{d1})$$
$$L\frac{di_q}{dt} = -Ri_q - \omega L i_d + (v_q - v_{q1}) \tag{2}$$

where ω is the synchronous angular speed of the fundamental system voltage.

Neglecting the voltage harmonics produced by the inverter, and according to the PWM technique, the voltage at the inverter output terminals and the DC-side can be written as:

$$v_{d1} = Kmv_{dc}\sin\alpha$$
$$v_{q1} = Kmv_{dc}\cos\alpha \tag{3}$$

where K is the inverter constant, which can be determined by the inverter structure, m is the modulation index of the PWM, v_{dc} is the DC-voltage across the STATCOM capacitor, and α is the firing angle that controls the power flow between the STATCOM and the PCC. m and α are the PWM control variables which given by

$$m = \frac{\sqrt{{v_{d1}}^2 + {v_{q1}}^2}}{Km}$$
$$\alpha = \tan^{-1}\frac{v_{q1}}{v_{d1}} \tag{4}$$

The instantaneous active and reactive power injected or absorbed at the PCC can be written as:

$$P = \frac{3}{2}(v_d i_d + v_q i_q)$$
$$Q = \frac{3}{2}(v_d i_q - v_q i_d) \tag{5}$$

while the instantaneous active power at the DC-side can be expressed as:

$$P = v_{dc} c \frac{dv_{dc}}{dt} \tag{6}$$

From equations (5) and (6), the dynamic equation for the DC-capacitor can be rewritten as a function of the STATCOM currents as follows:

$$\frac{dv_{dc}}{dt} = \frac{3}{2c}(v_d i_d + v_q i_q) \tag{7}$$

For simplification, the d-q coordinate frame is defined where d-axis is always coincident with the instantaneous voltage vector $v_q = 0$, and when $R \cong 0$, as a results the simplified model for the STATCOM, can be written as follows

$$L\frac{di_d}{dt} = \omega L i_q + (v_d - Kmv_{dc}\sin\alpha)$$
$$L\frac{di_q}{dt} = -\omega L i_d + Kmv_{dc}\cos\alpha \tag{8}$$

$$\frac{dv_{dc}}{dt} = \frac{3}{2c} v_d i_d \tag{9}$$

The reactive power is given by

$$Q = \frac{3}{2} v_d i_q \tag{10}$$

Therefore, the DC-voltage v_{dc} can be regulated by controlling i_d, and i_q which is sufficient to control the reactive power and hence the PCC voltage can be regulated.

The simplified model given by equations (8), and (9), is used along with the PI controller to regulate the PCC and the DC-capacitor voltages as shown in Fig. 3.

The PI controller parameters are selected using the robust optimization method Nelder and Mead [33, 34].

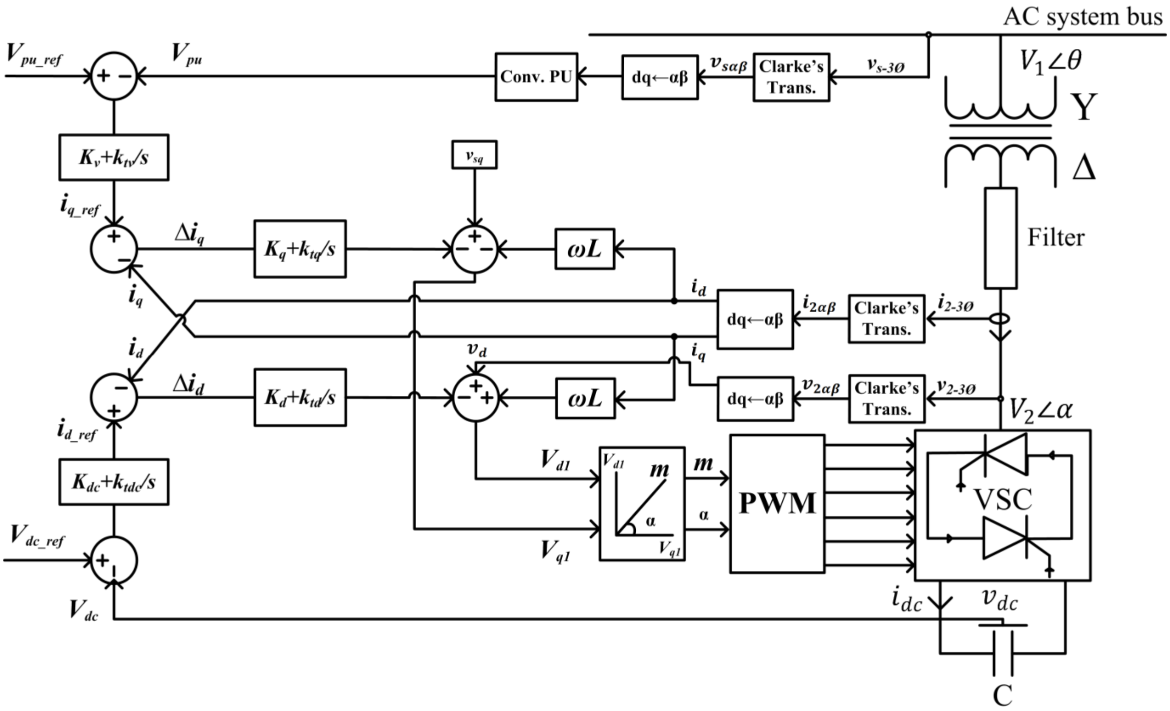

Fig. 3 The STATCOM controller.

IV. SIMULATION RESULTS

To study the impacts of the RSC fire-through fault on the voltage profile of the DFIG-based WECS, the system shown in Fig. 1 is simulated using EMTDC/PSCAD software. The DFIG is assumed to operate at unity power factor at wind speed of 11.5 m/s. The DFIG is initialized with a speed of 1.054 pu to pass the initial transient period, then switched to the torque control at t = 0.5s. The crowbar circuit is deactivated to study the impact of the fire-through fault on the dynamic performance of the DFIG-based WECS..

The STATCOM is connected to the PCC of the WECS and AC grid (bus-1 in Fig. 1). Time domain waveforms for the generator capacitor voltage, the rms rotor current, PCC reactive power, generator terminal voltage, and the STATCOM reactive power are investigated. Furthermore, the compliance of the voltage at the PCC of the WECS and the AC grid with various LVRT grid codes such as US, Spain, Mexico, Denmark, Germany, Quebec and UK [35, 36] with and without the proposed controller are examined and compared.

An intermittent fire-through of switch T3 of the RSC shown in Figs. 4 is assumed to take place at t = 6s and is assumed to last for 0.5 s. The impact of this fault on the WECS performance is elaborated in the below.

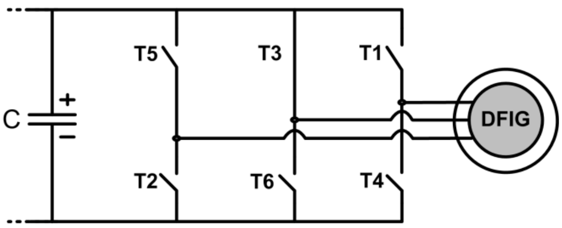

Fig. 4 The rotor side converter during the fire-through.

During the fault and by referring to Fig. 4, the DFIG experiences partial short circuit across rotor winding when switch T6 starts to conduct and the capacitor voltage will collapse to almost zero level as shown in Fig. 5. Due to the short circuit across rotor windings, rotor current increases to 1.5 pu as shown in Fig. 6. However this level is still within safe margins of 2 pu as specified in [37]. During fault, the DFIG absorbs a large amount of reactive power from the grid as shown in Fig. 7. After fault clearance the DFIG fails to retain the unity power factor operation and remains absorbing reactive power from the grid. With the connection of STATCOM, reactive power support will be delivered to the system as shown in Fig. 8. As a result, unity power factor operation can be retained after fault clearance and the reactive power requirement of the DFIG during the fault is significantly reduced as shown in Fig. 7. Fig. 9 shows that the DFIG terminal voltage experiences a voltage sag level of 20% of the nominal value during the fault and the generator voltage cannot be recovered after fault clearance. However, with the connection of the STATCOM and due to reactive power compensation, the voltage sag is reduced to only 3% during the fault and the voltage is recovered to its nominal steady state level after fault clearance.

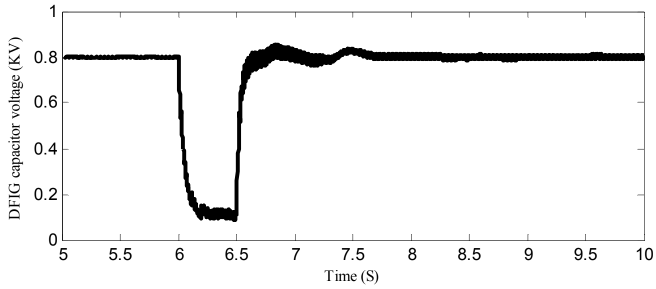

Fig. 5 The DFIG capacitor voltage.

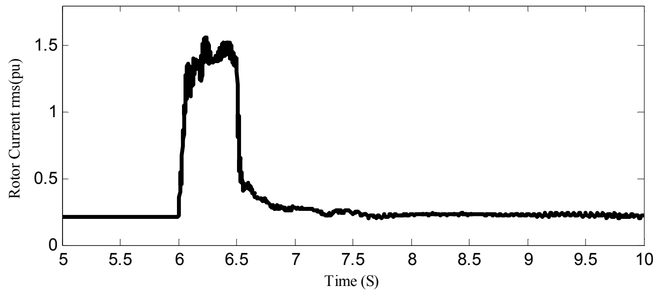

Fig. 6 The DFIG rms rotor current.

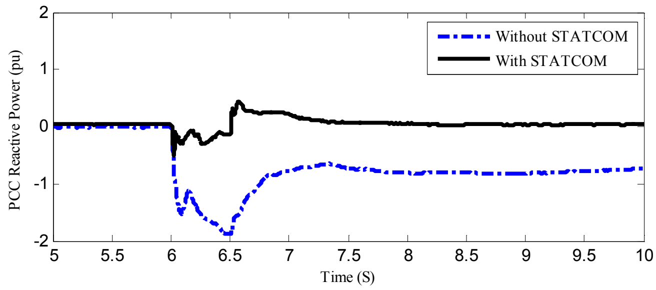

Fig. 7. PCC reactive power.

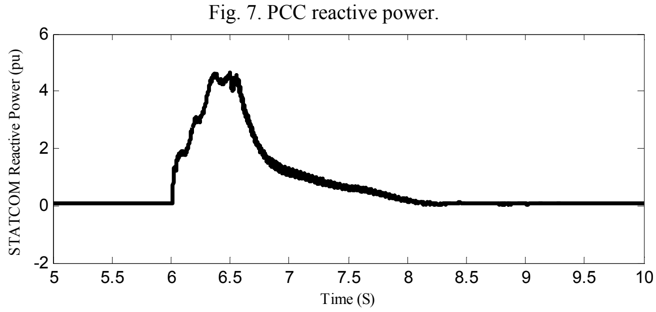

Fig. 8. The STATCOM reactive power.

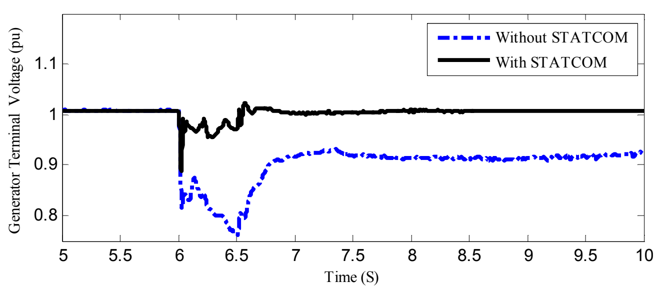

Fig. 9. Generator Terminal voltage.

The voltage at the PCC does not violate the LVRT of the all studied grid codes, however it will be on the margin of the lower level of the Denmark, Germany, US, and Ireland grid codes as shown in Fig. 10. The voltage recovery, due to the connection of the STATCOM, brings the voltage level to a safety level within all studied grid codes.

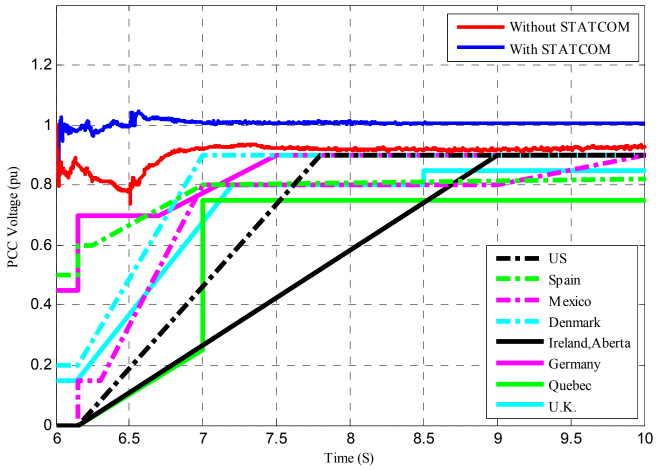

Fig. 10. PCC voltage compliance with various grid codes.

V. Conclusion

In this paper, a study has been performed to investigate the impact of the fire-through fault when takes place within the RSC of DFIG-based WECS on the converter capacitor voltage, the rms rotor current and the voltage profile of the DFIG. Compliance of the WECS under such fault with the LVRT of a various new grid codes is also investigated. Results show that the RSC fire-through has a critical impact on the overall performance of the WECS. A proper STATCOM controller is proposed to mitigate the impacts of the fault. Results show that the proposed controller is capable of bringing the voltage profile at the PCC to the nominal steady state level and maintaining the unity power factor operation of the DFIG during and after the fault duration.

References

[1] P. Musgrove, Wind Power. New York: Cambridge University Press, 2010.
[2] P. Van-Tung and L. Hong-Hee, "Performance Enhancement of Stand-Alone DFIG Systems With Control of Rotor and Load Side Converters Using Resonant Controllers," Industry Applications, IEEE Transactions on, vol. 48, pp. 199-210, 2012.
[3] T. Ackermann, Wind Power in Power System. West Sussex: John Wiley and Sons Ltd, 2005.
[4] M. Mohseni, S. M. Islam, and M. A. S. Masoum, "Impacts of Symmetrical and Asymmetrical Voltage Sags on DFIG-Based Wind Turbines Considering Phase-Angle Jump, Voltage Recovery, and Sag Parameters," Power Electronics, IEEE Transactions on, vol. 26, pp. 1587-1598, 2011.
[5] A. F. Abdou, A. Abu-Siada, and H. R. Pota, "Damping of subsynchronous oscillations and improve transient stability for wind farms," in Innovative Smart Grid Technologies Asia (ISGT), 2011 IEEE PES, 2011, pp. 1-6.
[6] A. Petersson and S. Lundberg, "Energy Efficiency Comparison of Electrical Systems for Wind Turbines," presented at the Nordic Workshop on Power and Industrial Electronics, Stockholm, Sweden 2002.
[7] C. Zhe, J. M. Guerrero, and F. Blaabjerg, "A Review of the State of the Art of Power Electronics for Wind Turbines," Power Electronics, IEEE Transactions on, vol. 24, pp. 1859-1875, 2009.
[8] W. Lixiang, R. J. Kerkman, R. A. Lukaszewski, L. Haihui, and Y. Zhenhuan, "Analysis of IGBT Power Cycling Capabilities Used in Doubly Fed Induction Generator Wind Power System," Industry Applications, IEEE Transactions on, vol. 47, pp. 1794-1801, 2011.
[9] C. Gang, H. Dan, M. Yun-Hui, C. Xiao, W. Tao, C. Xu, and L. Guo-Quan, "Transient Thermal Performance of IGBT Power Modules Attached by Low-Temperature Sintered Nanosilver," Device and Materials Reliability, IEEE Transactions on, vol. 12, pp. 124-132, 2012.
[10] H. B. A. Sethom and M. A. Ghedamsi, "Intermittent Misfiring Default Detection and Localisation on a PWM Inverter Using Wavelet Decomposition," Journal of Electrical Systems, vol. 4, 2008.
[11] F. W. Fuchs, "Some diagnosis methods for voltage source inverters in variable speed drives with induction machines - a survey," in Industrial Electronics Society, 2003. IECON '03. The 29th Annual Conference of the IEEE, 2003, pp. 1378-1385 Vol.2.
[12] Y. Shaoyong, A. Bryant, P. Mawby, X. Dawei, R. Li, and P. Tavner, "An Industry-Based Survey of Reliability in Power Electronic Converters," Industry Applications, IEEE Transactions on, vol. 47, pp. 1441-1451, 2011.
[13] J. Arrillaga, Y. H. Liu, and N. R. Watson, Flexible power transmission: the HVDC options: John Wiley, 2007.
[14] J. Arrillaga, High voltage direct current transmission: Institution of Electrical Engineers, 1998.
[15] L. Bin and S. K. Sharma, "A Literature Review of IGBT Fault Diagnostic and Protection Methods for Power Inverters," Industry Applications, IEEE Transactions on, vol. 45, pp. 1770-1777, 2009.
[16] K. R. Padiyar, HVDC power transmission systems: technology and system interactions: Wiley, 1990.
[17] L. Bin and S. Sharma, "A survey of IGBT fault diagnostic methods for three-phase power inverters," in Condition Monitoring and Diagnosis, 2008. CMD 2008. International Conference on, 2008, pp. 756-763.
[18] H. Sheng, L. Xinchun, K. Yong, and Z. Xudong, "An Improved Low-Voltage Ride-Through Control Strategy of Doubly Fed Induction Generator During Grid Faults," Power Electronics, IEEE Transactions on, vol. 26, pp. 3653-3665, 2011.
[19] A. O. Ibrahim, N. Thanh Hai, L. Dong-Choon, and K. Su-Chang, "A Fault Ride-Through Technique of DFIG Wind Turbine Systems Using Dynamic Voltage Restorers," Energy Conversion, IEEE Transactions on, vol. 26, pp. 871-882, 2011.
[20] A. Rolan, F. Corcoles, and J. Pedra, "Doubly Fed Induction Generator Subject to Symmetrical Voltage Sags," Energy Conversion, IEEE Transactions on, vol. 26, pp. 1219-1229, 2011.
[21] D. Campos-Gaona, E. L. Moreno-Goytia, O. Anaya-Lara, and G. Burt, "Ride-through-fault capabilities of DFIG wind farm connected to a VSC station during a DC fault," in AC and DC Power Transmission, 2010. ACDC. 9th IET International Conference on, 2010, pp. 1-5.
[22] L. Xin, Z. Tao, C. Yongning, and W. Weisheng, "Short Circuit Current Characteristic of Wind Generators," in Power and Energy Engineering Conference, 2009. APPEEC 2009. Asia-Pacific, 2009, pp. 1-4.
[23] R.-M. He, J.-L. Wang, J. Ma, Y.-H. Xu, and D. Han, "Impacts of DFIG-based wind farm on load modeling," in Power & Energy Society General Meeting, 2009. PES '09. IEEE, 2009, pp. 1-6.
[24] A. M. S. Yunus, M. A. S. Masoum, and A. Abu-Siada, "Application of SMES to Enhance the Dynamic Performance of DFIG During Voltage Sag and Swell," Applied Superconductivity, IEEE Transactions on, vol. PP, pp. 1-9, 2012.
[25] A. Abu-Siada and S. Islam, "Application of SMES Unit in Improving the Performance of an AC/DC Power System," Sustainable Energy, IEEE Transactions on, vol. 2, pp. 109-121.
[26] H. A. Darwish, A. M. I. Taalab, and M. A. Rahman, "Performance of HVDC converter protection during internal faults," in Power Engineering Society General Meeting, 2006. IEEE, 2006, p. 7.
[27] S. O. Faried and A. M. El-Serafi, "Effect of HVDC converter station faults on turbine-generator shaft torsional torques," Power Systems, IEEE Transactions on, vol. 12, pp. 875-881, 1997.
[28] K. R. Padiyar and A. M. Kulkarni, "Design of reactive current and voltage controller of static condenser," International Journal of Electrical Power & Energy Systems, vol. 19, pp. 397-410, 1997.
[29] A. F. Abdou, A. Abu-Siada, and H. R. Pota, "Application of a STATCOM for damping subsynchronous oscillations and transient stability improvement," in Universities Power Engineering Conference (AUPEC), 2011 21st Australasian, 2011, pp. 1-5.
[30] M. Khederzadeh, "Coordination control of statcom and ultc of power transformers," in Universities Power Engineering Conference, 2007. UPEC 2007. 42nd International, 2007, pp. 613-618.
[31] L. Shuhui and T. A. Haskew, "Analysis of Decoupled d-q Vector Control in DFIG Back-to-Back PWM Converter," in Power Engineering Society General Meeting, 2007. IEEE, 2007, pp. 1-7.
[32] R. Pena, J. C. Clare, and G. M. Asher, "Doubly fed induction generator using back-to-back PWM converters and its application to variable-speed wind-energy generation," Electric Power Applications, IEE Proceedings -, vol. 143, pp. 231-241, 1996.
[33] J. A. Nelder and R. Mead, "A Simplex Method for Function Minimization," The Computer Journal, vol. 7, pp. 308-313, January 1, 1965 1965.
[34] A. M. Gole, S. Filizadeh, and P. L. Wilson, "Inclusion of robustness into design using optimization-enabled transient simulation," Power Delivery, IEEE Transactions on, vol. 20, pp. 1991-1997, 2005.
[35] M. Tsili and S. Papathanassiou, "A review of grid code technical requirements for wind farms," Renewable Power Generation, IET, vol. 3, pp. 308-332, 2009.
[36] M. Altin, O. Goksu, R. Teodorescu, P. Rodriguez, B. B. Jensen, and L. Helle, "Overview of recent grid codes for wind power integration," in Optimization of Electrical and Electronic Equipment (OPTIM), 2010 12th International Conference on, 2010, pp. 1152-1160.
[37] M. Rahimi and M. Parniani, "Transient Performance Improvement of Wind Turbines With Doubly Fed Induction Generators Using Nonlinear Control Strategy," Energy Conversion, IEEE Transactions on, vol. 25, pp. 514-525, 2010.